recent microwave studies have revealed the production of the neutral SNS radical,[42] which would be isoelectronic with the highly stable radical ONO. Ab initio SCF MO calculations with configuration interaction predict that SNS is symmetric and bent with an SNS angle of 150° and a barrier of only about 3 kcal/mol to inversion through linear geometry.[43] According to Figure 4, eq 3 is symmetry allowed but eq 4 is forbidden. From the total energies in Table I, both dissociations appear to be endothermic:

$$\Delta E_3 = +21\ (6\text{-}31G^*/MP2),\ +24\ (6\text{-}31G^*),\ \text{or } +100\ \text{kcal/mol}\ (STO\text{-}3G^*)$$

$$\Delta E_4 = +36\ (6\text{-}31G^*/MP2),\ +50\ (6\text{-}31G^*),\ \text{or } +155\ \text{kcal/mol}\ (STO\text{-}3G^*)$$

Therefore, an extra electron makes $S_3N_2^+$ stable relative to dissociation compared to $S_3N_2^{2+}$.

(41) Matsumura, K.; Kawaguchi, K.; Nagai, K.; Yamada, C.; Hirota, E. *J. Mol. Spectrosc.* **1980**, *84*, 68.
(42) Amano, T.; Amano, T. reported in ref 43.
(43) Yamaguchi, Y.; Xie, Y.; Grev, R.S.; Schaefer, H. F., III *J. Chem. Phys.* **1990**, *92*, 3683.

Conclusions

Geometry optimized ab initio SCF MO calculations with STO-3G* and 6-31G* basis sets confirm that the ground state of $S_3N_2^+$ is $^2A_2$ as has been shown by ESR experiments. The calculated bond distances in $S_3N_2^+$ agree very well with those measured by X-ray crystallography. For the hypothetical neutral heterocycle S_3N_2, our calculations at the SCF level predict that the open-shell configuration $(2a_2)^1(3b_2)^1$ has lower energy than the closed-shell configurations $(2a_2)^2$ and $(3b_1)^2$, but MP2 correlation corrections reverse the order of the $^1A_1$ and $^3B_2$ states. The small splitting between the π levels $2a_2$ and $3b_1$ make this a close call. Optimized ab initio bond distances show differences between $S_3N_2^{2+}$, $S_3N_2^+$, and S_3N_2 in various electronic states that correlate with the qualitative model based on nodal properties of the $2a_2$ and $3b_1$ π MO's. Dissociation of $S_3N_2^{2+}$ into SN^+ and SNS^+ is favored by orbital symmetry and the nature of these fragments. A single electron in the $2a_2$ MO of $S_3N_2^+$ stabilizes this radical cation against dissociation.

Acknowledgment. We are grateful to the National Science Foundation for partial support of this research through Grant No. CHE-9012216 to the University of South Carolina.

Contribution from the Institut für anorganische Chemie, Universität Bern, Freiestrasse 3, CH-3000 Bern 9, Switzerland, and Laboratoire d'Optique Physique, ESPCI, 10, Rue Vauquelin, 75231 Paris Cedex 05, France

Double Excitations of $Ti^{2+}Mn^{2+}$ Spin Clusters in $MgCl_2$, $MnCl_2$, and $MnBr_2$

Markus Herren,[†] Michael A. Aebersold,[†] Bernard Briat,[‡] and Hans U. Güdel*,[†]

Received February 8, 1991

Blue-shifted sidebands on the well-known Mn^{2+} absorptions are observed in the visible absorption and MCD spectra of manganese chloride and bromide doped with Ti^{2+} and of magnesium chloride doped with both Ti^{2+} and Mn^{2+}. These sidebands are assigned to $Ti^{2+}Mn^{2+}$ double excitations of exchange-coupled Ti^{2+}-Mn^{2+} pairs ($MgCl_2$) and $Ti^{2+}(Mn^{2+})_6$ clusters ($MnCl_2$, $MnBr_2$), respectively. The energy differences ΔE of roughly 680 (chlorides) and 600 cm^{-1} (bromide) to the Mn^{2+} absorptions correspond to the trigonal splitting of the Ti^{2+} $^3T_{1g}(O_h)$ ground state. In the $^4A_{1g}{}^4E_g$ (Mn^{2+}) region, the absorption lines are sharp and ΔE in the visible absorption spectrum of $MgCl_2$:Ti^{2+},Mn^{2+} matches the known ground-state splitting of a Ti^{2+}-Mn^{2+} pair in $MgCl_2$. The trigonal ground-state splitting of Ti^{2+} in $MnBr_2$ has not been measured before. The principle of coupling an infrared electronic excitation on one ion with a visible excitation on a neighboring ion should be applicable to many other pairs of ions.

Introduction

Splittings of orbitally degenerate ground states of transition-metal ions in complexes and crystals resulting from low-symmetry ligand-field potentials and spin-orbit coupling are difficult to detect. They are often in the energy range 10-1000 cm^{-1}, which is not easily accessible by experiment. The magnetic susceptibility between 300 and 4 K may provide a rough estimate of the splitting.[1] Among the spectroscopic techniques that have been used to determine ground-state splittings, we mention infrared absorption spectroscopy,[2] electronic Raman spectroscopy,[3,4] and inelastic neutron scattering.[5] The latter two techniques have long been used to determine crystal-field splittings of rare-earth-metal ions in crystals.[6,7] We have recently found that luminescence spectroscopy provides a very accurate picture of the $^3T_{1g}$ ground-state splitting of Ti^{2+} and V^{3+} ions in various ionic lattices.[8,9]

In the present paper, we describe a principle by which a ground-state splitting can be made observable in the visible part of the absorption spectrum. We use Ti^{2+}-Mn^{2+} pairs in $MgCl_2$ and $Ti^{2+}(Mn^{2+})_6$ spin clusters in Ti^{2+}-doped $MnCl_2$ and $MnBr_2$ to illustrate both the principle and the effect. In these species, the Ti^{2+} and Mn^{2+} ions are coupled by exchange interactions. One of the consequences of exchange interactions is the occurrence of cooperative pair or cluster excitations, which have been studied for a long time.[10] The simultaneous excitation of a transition on two neighboring ions can lead to an absorption band at an energy corresponding roughly to the sum of the two single excitations.[11] In many cases, double excitations are observed in pairs of equal ions at twice the energy of single-ion ligand-field excitations.[12] By the same mechanism, two transitions with very different energies can also combine. In the present work, a transition within the energetically split $^3T_{1g}$ ground state of Ti^{2+} is added to a well-known ligand-field transition of Mn^{2+} in the blue spectral region.

The $^3T_{1g}$ (O_h) ground state of Ti^{2+} in the $MgCl_2$ and $MnCl_2$ lattices shows a large trigonal splitting ΔE of the order of 700 cm^{-1} into the components $^3A_{2g}$ and ^3E_g.[8] If a cooperative ab-

* Author to whom correspondence should be addressed.
† Universität Bern.
‡ ESPCI.

(1) Carlin, R. L. *Magnetochemistry*; Springer-Verlag: Heidelberg, Germany, 1986.
(2) Prinz, G. A. *Physica* **1977**, *89B*, 189.
(3) Clark, R. J. H.; Turtle, P. C. *Chem. Phys. Lett.* **1977**, *51*, 265.
(4) Lockwood, D. J.; Johnstone, I. W. *J. Appl. Phys.* **1982**, *53*, 8169.
(5) Furrer, A.; Wagner, V. *Verh. DPG (VI)* **1981**, *16*, 282.
(6) Amberger, H. D.; Rosenbauer, G. G.; Fischer, R. D. *Mol. Phys.* **1976**, *32*, 1291.
(7) *Proceedings of the Second International Conference on Crystal Field Effects in Metals and Alloys*; Furrer, A., Ed.; Plenum Press: New York, 1977.
(8) Jacobsen, S. M.; Güdel, H. U.; Daul, C. A. *J. Am. Chem. Soc.* **1988**, *110*, 7610.
(9) Reber, C.; Güdel, H. U. *J. Lumin.* **1988**, *42*, 1.
(10) Dexter, D. L. *Phys. Rev.* **1962**, *126*, 1962.
(11) Güdel, H. U. *Comments Inorg. Chem.* **1984**, *3*, 189.
(12) Riesen, H.; Güdel, H. U. *Mol. Phys.* **1987**, *60*, 1221.

0020-1669/91/1330-3280$02.50/0 © 1991 American Chemical Society

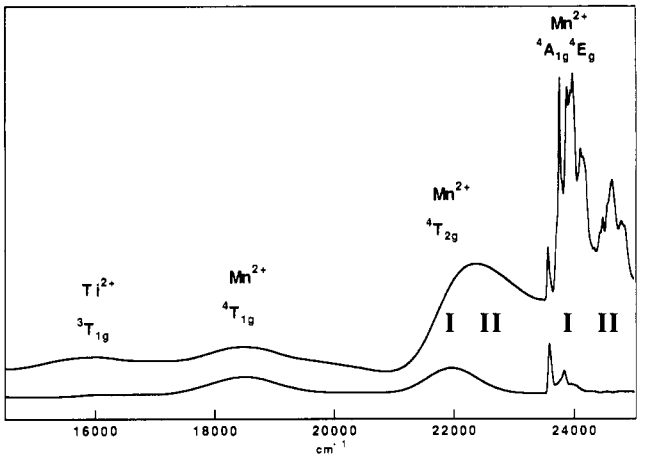

Figure 1. Survey absorption spectrum of $MnCl_2$:1% Ti^{2+} (top) and pure $MnCl_2$ (bottom) at 1.5 K. Band designations are given in octahedral notation; the labels I and II refer to the corresponding transitions in Figure 3.

sorption in Ti^{2+}–Mn^{2+} pairs or $Ti^{2+}(Mn^{2+})_6$ clusters involves a $^3A_{2g} \rightarrow {}^3E_g$ excitation on Ti^{2+}, we expect to see sidebands on the Mn^{2+} absorption bands that are blue-shifted by ΔE. In contrast to chlorides, ΔE in $MnBr_2$ has been unknown up to now.

Experimental Section

Single crystals of $MnBr_2$, $MnCl_2$, and $MgCl_2$ containing Ti^{2+} were grown in a Bridgman furnace at 800 °C, as described in ref 8. A crystal of $MgCl_2$:Ti^{2+} was doped in addition with Mn^{2+}, according to ref 13. All spectra were run with light propagating along the crystal c axis, perpendicular to the cleavage planes.[8] For magnetic circular dichroism (MCD) measurements, we used a homemade photoelastic modulator in conjunction with a phase-sensitive lock-in amplifier.[14] The samples were mounted in a liquid-helium-bath cryomagnet with a magnetic field up to 2 T. Absorption was measured either in the same experimental arrangement with a home-built double-beam attachment, or by a Cary 17 spectrometer with a closed-cycle helium refrigerator for sample cooling.

Results and Discussion

(a) $MgCl_2$ and $MnCl_2$. Figure 1 shows part of the low-temperature visible absorption spectrum of pure $MnCl_2$ and $MnCl_2$:1% Ti^{2+}. The doped crystal shows an enormous increase of the absorption intensity in the $^4T_{2g}$ and $^4A_{1g},{}^4E_g$ transitions on Mn^{2+}. This new intensity is due to $Ti^{2+}(Mn^{2+})_6$ spin cluster absorptions, and we observe that it is blue-shifted with respect to the $MnCl_2$ absorptions. In the $^4A_{1g},{}^4E_g$ region, the two bands I and II, corresponding to $^4A_{1g},{}^4E_g(Mn)^3A_{2g}(Ti)$ and $^4A_{1g},{}^4E_g(Mn)^3E_g(Ti)$ excitations, respectively, are resolved. This region is shown in greater detail in Figure 2. The traces A and B correspond to the MCD and absorption spectra of $MnCl_2$:1% Ti^{2+}, respectively. The origins of the two band systems I and II are more clearly identified in the MCD spectrum than in the absorption spectrum. Their energy separation ΔE is 678 cm^{-1}. The $^4A_{1g},{}^4E_g$ absorption spectrum of $MgCl_2$ doped with both Ti^{2+} and Mn^{2+} (Figure 2C) exhibits more fine structure, and the two band systems I and II are very well-defined. In this case, their origins are separated by 671 cm^{-1}, very close to the ΔE value found for the $Ti^{2+}(Mn^{2+})_6$ spin cluster. Figure 2D shows, for comparison, the luminescence spectrum of Ti^{2+}–Mn^{2+} pairs in $MgCl_2$.[15] The energy difference between the origins of the band systems III and IV, corresponding to $^1E_g \rightarrow {}^3A_{2g}(^3T_{1g})$ and $^1E_g \rightarrow {}^3E_g(^3T_{1g})$ Ti^{2+} emissions, respectively, equals 673 cm^{-1} and thus matches ΔE between I and II in Figure 2C almost exactly. Absorptions of trimers and higher clusters, which are also present in Figure 2C, can be ignored in the present discussion due to their lower intensity.[15] A diagram with all the relevant dimer states and the experimentally observed transitions is shown in Figure 3.

We emphasize the principle of observing a ground-state splitting as a sideband in the visible region in this paper. We ignore any additional splittings due to spin–orbit coupling, lower than trigonal point symmetry in Ti^{2+}–Mn^{2+} pairs, or exchange interactions of the states involved. For a more detailed analysis all these effects have to be taken into account.[15,16] Using the $^4A_{1g},{}^4E_g$ excitation of Mn^{2+}, we can obtain an excellent confirmation of the known trigonal ground-state splitting of Ti^{2+} in $MgCl_2$ and $MnCl_2$. This is due to the sharpness of the $^6A_{1g} \rightarrow {}^4A_{1g},{}^4E_g$ transitions on Mn^{2+}, which occur within the $(t_{2g})^3(e_g)^2$ configuration. The $^3A_{2g} \rightarrow {}^3E_g$

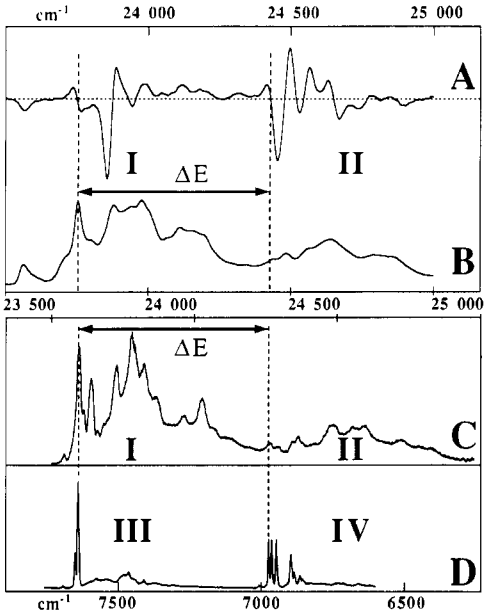

Figure 2. $^4A_{1g},{}^4E_g$ region (Mn^{2+}) in $MnCl_2$:1% Ti^{2+} at 2 K ((A) MCD spectrum; (B) absorption spectrum) and $MgCl_2$:2% Ti^{2+}, 15% Mn^{2+} at 22 K ((C) absorption spectrum) and (D) near-IR emission of selectively excited $Mn^{2+}Ti^{2+}$ pairs in $MgCl_2$ at 5 K.[15] The labels I, II, III, and IV refer to the corresponding transitions in Figure 3. Note that the energy scale of spectrum C is shifted by 160 cm^{-1} to lower energy with respect to spectra A and B.

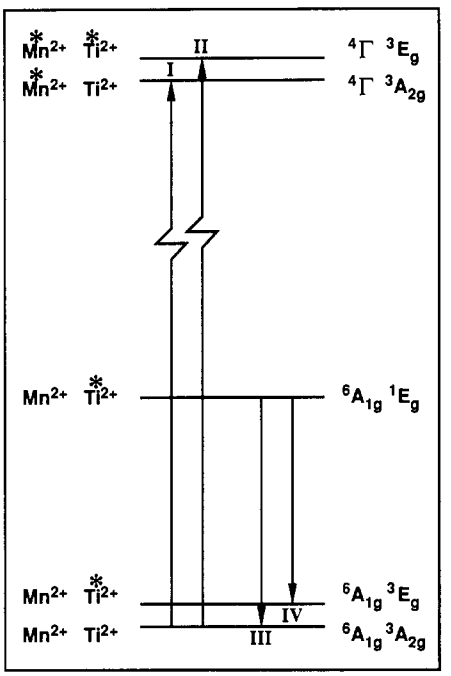

Figure 3. Relevant excited states of Ti^{2+}–Mn^{2+} pairs in $MgCl_2$ and observed spectroscopic transitions. Ions in an excited state are marked by an asterisk.

(13) Herren, M.; Jacobsen, S. M.; Güdel, H. U. *Inorg. Chem.* **1989**, *28*, 504.
(14) Canit, J. C.; Badoz, J. *Appl. Opt.* **1984**, *23*, 2861.
(15) Herren, M.; Jacobsen, S. M.; Güdel, H. U.; Briat, B. *J. Chem. Phys.* **1989**, *90*, 663.
(16) Aebersold, M. A.; Blank, H.; Briat, B.; Furrer, A.; Güdel, H. U. *Inorg. Chem.*, in press.

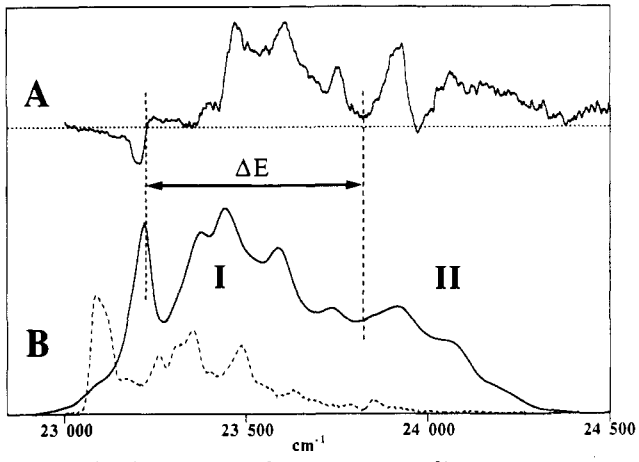

Figure 4. $^4A_{1g}{}^4E_g$ region (Mn^{2+}) in $MnBr_2$:5%Ti^{2+} at 4.2 K: (A) MCD spectrum; (B) absorption spectrum (solid line). The dashed line represents the absorption spectrum of pure $MnBr_2$ at 4.2 K with expanded (factor of 5) ordinate scale.

transition on Ti^{2+} is also intraconfigurational, within $(t_{2g})^2$, and thus the double excitations in the Ti^{2+}–Mn^{2+} pairs and Ti^{2+}-$(Mn^{2+})_6$ clusters are also observed as sharp absorption bands. The situation is different for the $^4T_{2g}$ transition in Mn^{2+}. Due to its intrinsic broadness, bands I and II are not resolved and we only observe a blue-shift and an asymmetric shape of the corresponding absorption band; see Figure 1. Note that the $^4T_{1g}$ transition on Mn^{2+} neither is enhanced in $MnCl_2$:Ti^{2+} nor shows a blue-shift. Exchange interactions between Ti^{2+} and Mn^{2+} are evidently much less efficient in inducing intensity for this transition.

(b) $MnBr_2$. The two band systems I and II for the $^4T_{2g}$ and $^4A_{1g}{}^4E_g$ excitations of Mn^{2+} are also observed in the absorption and MCD spectra of $MnBr_2$:Ti^{2+}, but not as clearly separated from each other as in the chlorides. Figure 4 shows the $^4A_{1g}{}^4E_g$ region in comparison with the absorption spectrum of pure $MnBr_2$. The energy separation ΔE, corresponding to the trigonal Ti^{2+} ground-state splitting, is roughly 600 cm^{-1}. In this case, ΔE is not accessible by luminescence spectroscopy, because Ti^{2+} does not show sharp emission lines in bromide lattices.[8]

Conclusion

The principle of coupling an infrared electronic excitation on one ion with a visible excitation on a neighboring ion, thus producing an easily detectable sideband in the absorption spectrum of the latter, should be applicable to many other pairs of ions. The best results can be expected in those cases in which the visible absorption corresponds to a sharp-band intraconfigurational transition.

Acknowledgment. This work was financially supported by the Swiss NSF and the French CNRS.

Registry No. $MnCl_2$, 7773-01-5; $MnBr_2$, 13446-03-2; $MgCl_2$, 7786-30-3; Ti^{2+}, 15969-58-1; Mn^{2+}, 16397-91-4.

Contribution from the Institute for Molecular Science, Myodaiji, Okazaki 444, Japan, and Department of Applied Chemistry, Faculty of Engineering, Osaka University, Yamada-oka, Suita, Osaka 565, Japan

Electrochemical Assimilatory and Dissimilatory Reductions of NO_3^- and NO_2^- via a Possible Free NO Intermediate

Koji Tanaka,*[†] Nobutoshi Komeda,[‡] and Tatsuji Matsui[‡]

Received August 24, 1990

Both NO_3^- and NO_2^- were selectively reduced to NH_3 by a $(Bu_4N)_4[MoFe_3S_4(SPh)_3(O_2C_6Cl_4)]_2$-modified glassy-carbon electrode ($[MoFe_3S_4]$/GC) under controlled-potential electrolysis at −1.25 V vs SCE in H_2O (pH 10.0), while NO_2^- was reduced predominantly to N_2 by the same electrode under electrolysis at −1.00 V. Nitrite ion preferentially binds to molybdenum of the $[MoFe_3S_4]$/GC with the oxygen atom, where either bound or terminal oxygen of the Mo–ONO^- moiety is removed by reduction. An electrochemical study indicates the presence of free NO as the common reaction intermediate in these assimilatory and dissimilatory reductions of NO_2^-.

Introduction

Dissimilatory and assimilatory reductions of NO_3^- and NO_2^- are the key reactions in the nitrogen cycle. Although the details of these enzymatic reductions have not been fully elucidated so far, it is generally believed that NO_3^- is first reduced to NO_2^- by molybdenum-containing nitrate reductases,[1] and then NO_2^- is reduced to NH_3 via nitrosyl and hydroxylamine by assimilatory nitrite reductases containing sirohemes.[2] On the other hand, dissimilatory nitrite reductases containing hemes *c* and d_1[3] reduce NO_2^- to N_2O, which is further reduced to N_2.[4] The N–N bond formation in the dissimilatory reduction of NO_2^- is currently a matter of controversy; generally accepted pathways from NO_2^- to N_2O are either nucleophilic attack of NO_2^- on E-NO^+ generated by an acid–base equilibrium reaction of enzyme-bound NO_2^- (E-NO_2^-)[5] or dimerization of HNO (or NO^-) resulting from two-electron reduction of NO_2^-.[6] Evolution of low levels of NO from nitrite reductases,[7] however, further complicates these pathways since the affinity of heme protein for NO is very strong[8]

[†] Institute for Molecular Science.
[‡] Osaka University.

(1) (a) Payne, W. J. *Denitrification*; Wiley-Interscience: New York, 1981; p 214. (b) Adams, M. W. W.; Mortenson, L. E. *Molybdenum Enzymes*; Spiro, T. G., Ed.; Wiley-Interscience: New York, 1985; pp 519–593.
(2) (a) Vega, J. M.; Kamin, H. *J. Biol. Chem.* **1977**, *252*, 896. (b) Murphy, M. J.; Siegel, L. M.; Tove, S. R.; Kamin, H. *Proc. Natl. Acad. Sci. U.S.A.* **1974**, *71*, 612.
(3) (a) Timkovich, R.; Cork, M. S.; Taylor, P. V. *J. Biol. Chem.* **1984**, *259*, 1577. (b) Timkovich, R.; Dhesi, R.; Martinkus, K. J.; Robinson, M. K.; Rea, T. M. *Arch. Biochem. Biophys.* **1982**, *215*, 47.
(4) Henry, Y.; Bessieres. *Biochimie* **1984**, *66*, 259.
(5) (a) Garber, E. A. E.; Hollocher, T. C. *J. Biol. Chem.* **1982**, *257*, 8091. (b) Weeg-Aerssens, E.; Tiedje, J. M.; Averill, B. A. *J. Am. Chem. Soc.* **1988**, *110*, 6851. (c) Aerssens, E.; Tiedje, J. M.; Averill, B. A. *J. Biol. Chem.* **1986**, *261*, 9652. (d) Averill, B. A.; Tiedje, J. M. *FEBS Lett.* **1982**, *138*, 8.
(6) (a) Kim, C.-H.; Hollocher, T. C. *J. Biol. Chem.* **1984**, *259*, 2092. (b) Garber, E. A. E.; Hollocher, T. C. *J. Biol. Chem.* **1982**, *257*, 4705. (c) Kim, C.-H.; Hollocher, T. C. *J. Biol. Chem.* **1983**, *258*, 4861. (d) Garber, E. A. E.; Wehrli, S.; Hollocher, T. C. *J. Biol. Chem.* **1983**, *258*, 3587.

0020-1669/91/1330-3282$02.50/0 © 1991 American Chemical Society